



# The effect of three dental cement types on the corrosion of dental implant surfaces

Mostafa Alhamad<sup>a,\*</sup>, Valentim A.R. Barão<sup>b</sup>, Cortino Sukotjo<sup>c</sup>, Mathew T. Mathew<sup>c</sup>

<sup>a</sup> Department of Restorative Dental Sciences, College of Dentistry, Imam Abdulrahman Bin Faisal University, Dammam, Saudi Arabia

<sup>b</sup> Department of Prosthodontics and Periodontology, Piracicaba Dental School, University of Campinas (UNICAMP), Piracicaba, São Paulo, Brazil

<sup>c</sup> Department of Restorative Dentistry, College of Dentistry, University of Illinois Chicago, Chicago, IL, USA

## ARTICLE INFO

### Keywords:

Titanium  
Corrosion  
Peri-implantitis  
Dental cement

## ABSTRACT

**Statement of problem:** One of the main challenges facing dental implant success is peri-implantitis. Recent evidence indicates that titanium (Ti) corrosion products and undetected-residual cement are potential risk factors for peri-implantitis. The literature on the impact of various types of dental cement on Ti corrosion is very limited.

**Purpose:** This study aimed to determine the influence of dental cement on Ti corrosion as a function of cement amount and type.

**Materials and methods:** Thirty commercially pure Ti grade 4 discs (19 × 7mm) were polished to mirror-shine (Ra ≈ 40 nm). Samples were divided into 10 groups (n = 3) as a cement type and amount function. The groups were no-cement as control, TempBond NE (TB3mm, TB5mm, and TB8mm), FujiCEM-II (FC3mm, FC5mm, and FC8mm), and Panavia-F-2.0 (PC3mm, PC5mm, and PC8mm). Tafel's method estimated corrosion rate ( $i_{\text{corr}}$ ) and corresponding potential ( $E_{\text{corr}}$ ) from potentiodynamic curves. Electrochemical Impedance Spectroscopy (EIS) data was utilized to obtain Nyquist and Bode plots. An equivalent electrical circuit estimated polarization resistance ( $R_p$ ) and double-layer capacitance ( $C_{\text{dl}}$ ). Inductively coupled plasma mass spectrometry (ICP-MS) analysis was conducted to analyze the electrolyte solution after corrosion. pH measurements of the electrolyte were recorded before and after corrosion tests. Finally, the corroded surface was characterized by a 3D white-light microscope and scanning electron microscope. Statistical analysis was conducted using either one-way ANOVA followed by Tukey's Post Hoc test or Kruskal-Wallis followed by Dunn's test based on data distribution.

**Results:** Based on cement amount, FC and PC significantly increased  $i_{\text{corr}}$  in higher amounts (FC8mm- $i_{\text{corr}}$  =  $8.22 \times 10^{-8}$  A/cm<sup>2</sup>, PC8mm- $i_{\text{corr}}$  =  $5.61 \times 10^{-8}$  A/cm<sup>2</sup>) compared to control ( $3.35 \times 10^{-8}$  A/cm<sup>2</sup>). In contrast, TB3mm decreased  $i_{\text{corr}}$  significantly compared to the control. As a function of cement type, FC increased  $i_{\text{corr}}$  the most. EIS data agrees with these observations. Finally, corroded surfaces had higher surface roughness (Ra) compared to non-corroded surfaces.

**Conclusion:** The study indicated that cement types FC and PC led to increased Ti-corrosion as a function of a higher amount. Hence, the implant stability could be impacted by the selection, excessive cement, and a potentially increased risk of peri-implantitis.

\* Corresponding author.

E-mail addresses: [mtalhamad@iau.edu.sa](mailto:mtalhamad@iau.edu.sa) (M. Alhamad), [vbarao@unicamp.br](mailto:vbarao@unicamp.br) (V.A.R. Barão), [csukotjo@uic.edu](mailto:csukotjo@uic.edu) (C. Sukotjo), [mtmathew@uic.edu](mailto:mtmathew@uic.edu) (M.T. Mathew).

<https://doi.org/10.1016/j.heliyon.2023.e23626>

Received 7 May 2023; Received in revised form 23 November 2023; Accepted 8 December 2023

Available online 16 December 2023

2405-8440/© 2023 Published by Elsevier Ltd.

This is an open access article under the CC BY-NC-ND license

(<http://creativecommons.org/licenses/by-nc-nd/4.0/>).

## 1. Introduction

Based on the 2017 World Workshop on Peri-Implantitis [1], the most significant risk factor/indicator for peri-implantitis is dental plaque, which builds up in the absence of proper oral hygiene. In addition, smoking, a history of periodontitis, and systemic factors such as uncontrolled diabetes are risk factors/indicators for peri-implantitis. Recently suggested are other risk factors, including Ti ions and particles (products of corrosion and wear, respectively) [2–6], and undetected excess cement in the peri-implant tissues [7–10], Titanium is the most commonly used material in the fabrication of dental implants, because of its high biocompatibility due to the instant formation of projective oxide layer. Nevertheless, Ti implants can encounter a severe corrosion-promoting environments in the oral cavity [11]. Ti corrosion acceleration can be a result of eating foods with high electrolyte content, pH drop from citrus foods and beverages, and/or poor oral hygiene that results in increased bacterial products such as lipopolysaccharides [12,13]. Higher amount of Ti particles/ions were detected around implants with peri-implantitis, when compared to healthy implant sites [5,14]. In the literature, several Ti corrosion mechanisms in the oral environment have been reported, which include electrochemically-induced mechanism, such as pitting and crevice corrosion, mechanically-induced mechanisms such as fretting corrosion (as a result of micromovements), and combined electrochemical and mechanical mechanisms, which is termed as tribocorrosion [15].

In implant dentistry, the implant crown can be retained with a screw (screw-retained) or cement (cement-retained). The advantages of cement-retained implant crowns include esthetics, compensation for unfavorable implant angulation, and ease of fabrication in the dental lab [16]. Thus, cement-retained implant crowns are commonly used in dentistry. In 2017, Makke et al. surveyed the frequency of cement-retained and screw-retained crown use. They found that 83% (a total of 83 dentists) used cement-retained crowns as opposed to screw-retained [16]. In a cross-sectional analysis investigating peri-implant disease in 225 implants, Daubert and coauthors reported that 69.4% of the implant restorations were cement-retained, indicating that the use of this crown option is common [17]. Another study in 2018 looking at implant-supported prosthesis complications based on the records of 2666 patients reported that 32% of restorations were cement-retained [18].

One of the main disadvantages of cement-retained implant crowns is the high risk of undetected excess cement, even with meticulous cement removal in some cases [7]. This residual cement is a potential risk indicator/factor for peri-implantitis. The literature reported that residual cement was associated with bleeding on probing and suppuration [7,9]. Wilson et al. found bleeding on probing in 80% of implants with undetected excess cement and suppuration in 20% of implants [9]. In a retrospective study, Korsch et al. recalled 171 implants with cement-retained restoration, in which methacrylate cement was used, and found increased signs of inflammation were associated with undetected excess cement [19]. In another study, Korsch et al. reported that signs of inflammation were associated with methacrylate-based cement, even in the absence of residual cement [8].

In addition to potentially increasing the risk of peri-implantitis, some types of dental cement could accelerate Ti corrosion [20,21]. In 2017, Saba and coauthors investigated the impact of 4 dental cement types on grade 2 commercially pure Ti surface corrosion. They found that Cermair cement (nano-structurally integrating bioceramic) increased the corrosion rate the most, and Premier implant cement (resin-based) had the least corrosion rate. The authors explained that the fluoride content of Cermair cement is the potential cause of corrosion increase [22]. In implant dentistry, applying sufficient amount of cement within the implant restoration can be difficult for some clinicians without proper training, which can increase the risk of undetected residual cement [23]. A survey involving around 400 dentists showed a lack of standardization for the amount of cement used [24]. This could lead to variable amounts of undetected excess cement in contact with the implant surface. To the best of our knowledge, the effect of the amount of cement on Ti corrosion has never been studied; therefore, this study aimed to determine the influence of dental cement on Ti corrosion as a function of cement amount and type. The first hypothesis is that the cement amount produces Ti corrosion. The second hypothesis is that the cement type influences Ti corrosion.

## 2. Materials and methods

### 2.1. Sample preparation

Thirty commercially pure titanium grade 4 discs (19 mm in diameter and 7 mm in thickness) were obtained by sectioning a Ti bar (Supra Alloys). The Ti discs were divided into 10 groups as a function of cement type and amount. The groups are summarized in Table 1. The Ti samples were ground sequentially with 320-, 400-, 600- and 800-grit silicon carbide grinding papers (Carbimet 2, Buehler). Afterward, the samples were polished with a polishing cloth (TextMet Polishing Cloth, Buehler) on which diamond paste (MetaDi 9- $\mu$ m, Buehler) was suspended in lubricant (MetaDi Fluid, Buehler). Finally, the polishing was finalized with a polishing cloth (Chemomet I, Buehler) and colloidal silica polishing suspension (MasterMed, Buehler) (Ra  $\approx$  40 nm). Before all tests, the samples were sonicated in distilled water and 70% propanol for 10 min each.

**Table 1**  
The details of the groups of the current study.

Group abbreviations	Cement type (amount)
C	No cement
TB	Tempbond cement in three different amounts, 3 mm (TB3mm), 5 mm (TB5mm), and 8 mm (TB8mm)
FC	FujiCEM II in three different amounts, FC3mm, FC5mm, and FC8mm
PC	Panavia F 2.0 in three different amounts, PC3mm, PC5mm, and PC8mm

## 2.2. Electrolyte and cement preparation

The electrolyte solution used in all corrosion experiments was freshly prepared artificial saliva with the following composition added to distilled water; KCl (0.4 g/L), NaCl (0.4 g/L), CaCl<sub>2</sub>·2H<sub>2</sub>O (0.906 g/L), NaH<sub>2</sub>PO<sub>4</sub>·2H<sub>2</sub>O (0.690 g/L), urea (1 g/L), and Na<sub>2</sub>S·9H<sub>2</sub>O (0.005 g/L). After that, the physiologic pH of 6.5 was obtained, primarily by adding sodium hydroxide.

In this study, three cement types with variable micro-shear strengths were selected, which are commonly used in implant dentistry. The cement types are TempBond NE (Kerr Corporation), FujiCEM II (GC America Inc.), and Panavia F 2.0 (Kuraray America Inc.) (Table 2). To minimize the inconsistencies in the amount of cement within each group, a mold was made using a polyvinylsiloxane impression material (Extrude Medium, Kerr Corporation), and punched in the center with a 3 mm-, 5 mm-, or 8 mm-punch biopsy tool (Miltex Biopsy Punch) (Fig. 1A) to ultimately obtain three amounts of dental cement. Each cement was prepared following the manufacturer's instructions, and an additional 5 min was given to ensure complete cement setting before initiating the electrochemical tests. After complete setting, the cement adhered to the top of Ti sample (Fig. 1A).

## 2.3. Electrochemical tests

Fig. 1B demonstrates the electrochemical setup used in the current study. All electrochemical tests were performed using a three-electrode system following the American Society for Materials and Testing guidelines (G-61). The electrodes were a counter electrode (graphite), a reference electrode (saturated calomel-SCE), and a working electrode, which is the exposed area of the sample in contact with the electrolyte solution. The exposed area of control (no cement) was 1.22 cm<sup>2</sup>. For the other groups, the cement was applied on top of the Ti sample, which reduced the exposed area of Ti as the amount of cement increased (1.15 cm<sup>2</sup> in 3 mm groups, 1.02 cm<sup>2</sup> in 5 mm groups, and 0.717 cm<sup>2</sup> in 8 mm groups). The tests were performed using a customized polysulfone corrosion cell and a physiologic temperature (37 °C) was maintained throughout the tests. A potentiostat (G300, Gamry inc.) was used to conduct corrosion tests. The corrosion sequence started with an open circuit potential (OCP) (300 s) and potentiostatic steps (PS) (600 s) for electrochemical cleaning, followed by another OCP for 3600 s. After that, the electrochemical impedance spectroscopy (EIS) was achieved with a starting frequency of 100 kHz and an ending frequency of 0.005 Hz at open circuit potential (E<sub>oc</sub>). From EIS data, Nyquist and bode plots were drawn, and a modified Randle's circuit was applied, from which polarization resistance (R<sub>p</sub>) and double-layer capacitance (C<sub>dl</sub>) were estimated. Following is the potentiodynamic step with a potential starting from -0.8 V to 1.8 V and 1.8 V to -0.8 V versus SCE. The current density (i<sub>corr</sub>) and corresponding potential (E<sub>corr</sub>) were calculated using Tafel's method.

## 2.4. Inductively coupled plasma mass spectrometry (ICP-MS)

To quantify the amount of Ti and Zn ions in the electrolyte solution following the corrosion tests, ICP-MS analysis was performed for each sample after corrosion. The elemental tests were performed at the Northwestern University Quantitative Bio-element Imaging Center.

## 2.5. pH measurement

To determine the pH change over time, each cement was placed in fresh artificial saliva for 4 h, and the pH was measured at different time points, baseline, 30 min, 1 h, 2 h, and 4 h. The 5-mm mold was used to control the amount of cement. The cement was placed in the artificial saliva 5 min after the setting time, and measurements were taken at room temperature.

**Table 2**  
Cement types used in this study and their compositions.

Cement (Manufacturer)	Component (Lot number)	Composition	Curing mode/Setting time
TempBond NE (Kerr Corporation)	Base (8081977)	Zinc oxide (60–100%), White mineral oil (petroleum) (5–10%)	Self-cure/4 min
	Catalyst (8081977)	Octanoic acid (10–30%), 2-ethoxybenzoic acid (10–30%), (R)- <i>p</i> -mentha-1,8-diene (0.1–1%)	
FujiCEM II (GC America Inc.)	Paste A (2203222)	Alumino-fluoro-silicate glass (amorphous), hydroxyethyl methacrylate, Dimethacrylate, Bis-MEPP, Silicon Dioxide, pigment	Self-cure/4.5 min
	Paste B (2203222)	Polyacrylic acid, distilled water, silicone dioxide, initiator	
Panavia F 2.0 (Kuraray America Inc.)	Paste A (5D0249)	10-Methacryloyloxydecyl dihydrogen phosphate, hydrophobic aromatic dimethacrylate, hydrophobic aliphatic dimethacrylate, hydrophilic aliphatic dimethacrylate, silanated silica filler, silanated colloidal silica, DL-Camphorquinone, Catalysts	Dual-cure/light cure for 20 s or 3-min setting time when isolated from air
	Paste B (CH0106)	Hydrophobic aromatic dimethacrylate, hydrophobic aliphatic dimethacrylate, hydrophilic aliphatic dimethacrylate, silanated barium glass filler, catalysts, accelerators, pigments	

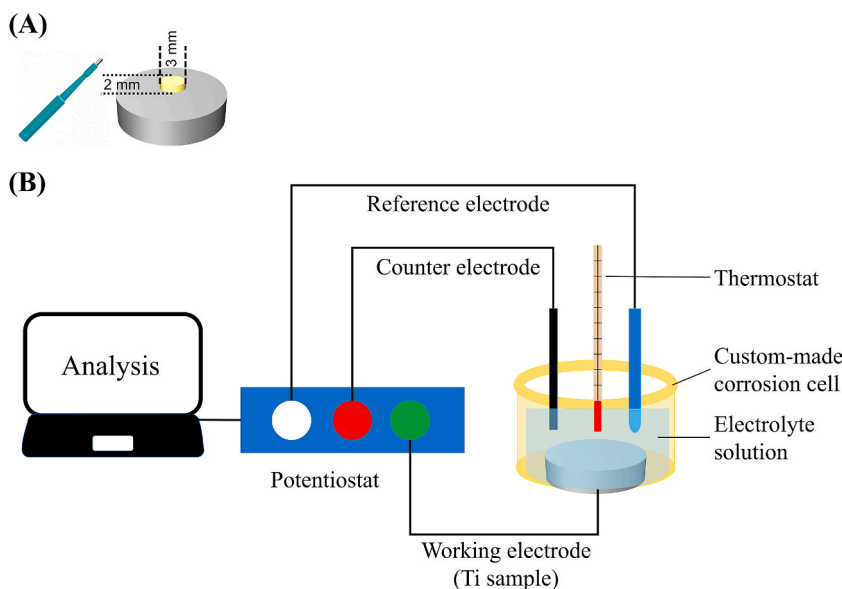


**Fig. 1.** A, Method used to control the cement amount in this study. Polyvinylsiloxane molds were punched in the center with a 3 mm-, 5 mm-, or 8 mm-punch biopsy tool (left image) to obtain reproducible cement cylinder with a 3 mm-, 5 mm-, or 8 mm-diameter and 2 mm thickness. B, Schematic diagram of the electrochemical setup.

## 2.6. Surface analysis

The change in the corroded surfaces compared to non-corroded surfaces was analyzed with a 3D-white light microscope (Bruker-Nano Contour GT-K Optical Profilometer). Surface roughness ( $R_a$ ) measurements were taken before and after corrosion using this microscope. Furthermore, the corroded and non-corroded surfaces were examined under a scanning electron microscope (SEM) (Jeol JSM-IT500HR, Oxford Instruments) to further check the surface quality under high magnification ( $3000\times$ ). The change in the surface chemical elements was examined with energy dispersive spectroscopy (EDS).

## 2.7. Statistical analysis

The statistical analysis started by checking the data distribution using Shapiro Wilk normality test. One-way ANOVA followed by Tukey's Post Hoc test was performed for parameters with normally distributed data. Kruskal-Wallis followed by Dunn's test, were used in the case of non-normally distributed data. The variables were  $i_{\text{corr}}$ ,  $E_{\text{corr}}$ ,  $R_p$ ,  $C_{dl}$  and were compared to the control. For ICP-MS data, Pearson's correlation was performed for the amount of cement and concentration of Ti and Zn. The power analysis was performed with a confidence level of 5%. All statistical tests were achieved with SPSS 28.0.0.0.

## 3. Results

### 3.1. Open circuit potential (OCP)

The OCP curves illustrate the corrosion thermodynamic tendency of the material. A higher OCP value indicates less corrosion tendency, while a lower OCP value indicates a higher corrosion tendency. Based on OCP curves of the TB groups (Fig. 2A), TB cement in different amounts decreased the OCP compared to control, indicating more corrosion tendency (TB groups OCP range =  $-0.3$  to  $-0.5$  V versus SCE, control OCP =  $-0.2$  V versus SCE). Similarly, FC (Fig. 2B) and PC (Fig. 2C) groups dropped the OCP value compared to the control, with FC and PC groups OCP ranging between  $-0.3$  and  $-0.5$  V versus SCE. As a function of cement type, all cement types reduced the OCP compared to the control (Fig. 2D).

### 3.2. Potentiodynamic curves

The potentiodynamic curves are used to determine the corrosion behavior of the material in terms of corrosion potential and density. Figs. 3 and 4 present the potentiodynamic curves generated in this study. TB generally reduced  $i_{\text{corr}}$  compared to control, with a statistically significant decrease in group TB3 ( $P = .043$ ) (Fig. 3A). In contrast, all amounts of FC increased  $i_{\text{corr}}$  in comparison to the control, which was statistically significant in groups FC5mm and FC8mm ( $P \leq .001$ ) (Fig. 3B). When PC was added in three different amounts, only PC5mm and PC8mm increased  $i_{\text{corr}}$  as opposed to the control, with the latter having a statistical significance ( $P \leq .001$ ) (Fig. 3C). Regarding  $E_{\text{corr}}$ , FC5mm and FC8mm decreased it significantly ( $P = .02$ ), indicating more corrosion tendency, and all the

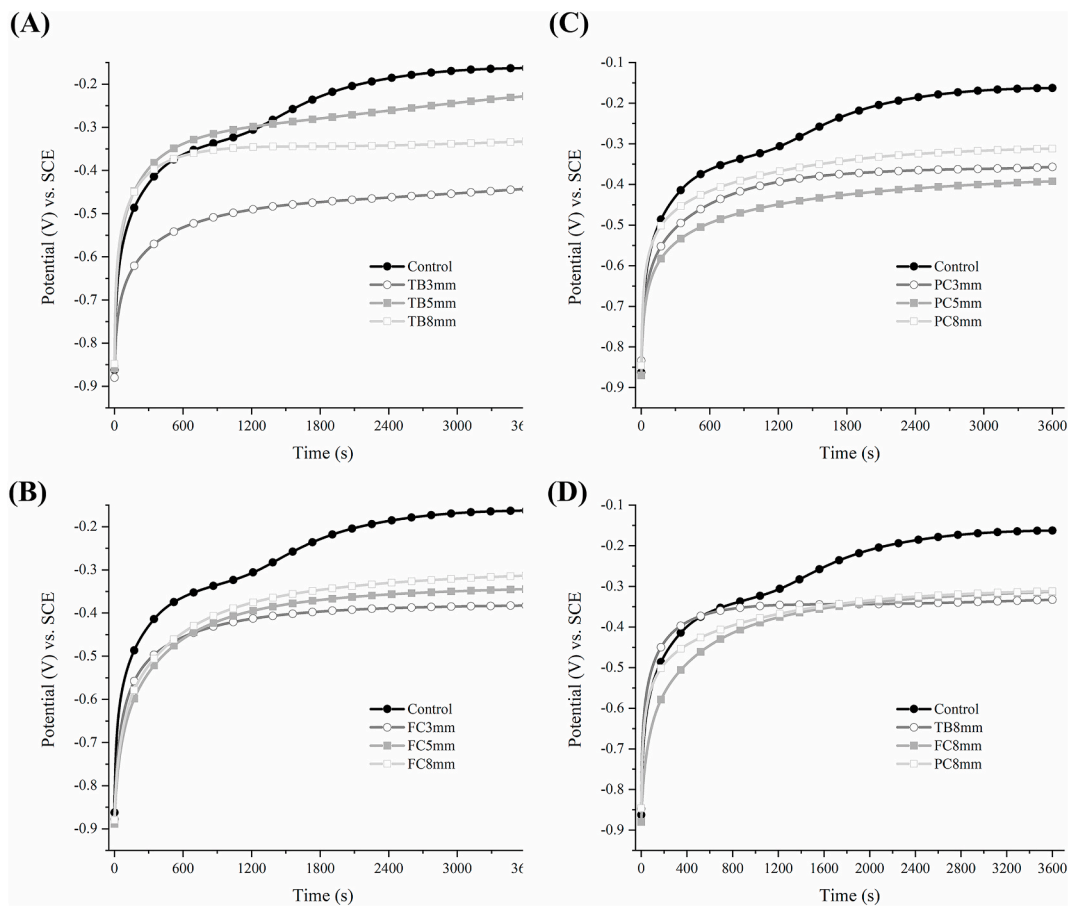


**Fig. 2.** A-C, OCP curves as a function of cement amount, and D, as a function of cement type. Generally, a lower OCP indicates higher corrosion tendency.

other groups had statistically similar  $E_{\text{corr}}$  to control at  $p = .05$  (Fig. 3). Table 3 demonstrates means and standard deviations of  $i_{\text{corr}}$  and  $E_{\text{corr}}$  in this study.

As a function of cement type (Fig. 4), FC increased  $i_{\text{corr}}$  the most, followed by PC ( $P \leq .05$ ), while TB slightly decreased  $i_{\text{corr}}$  compared to the control (Fig. 4B).  $E_{\text{corr}}$  dropped significantly by FC ( $P \leq .05$ ), while TB and PC had similar  $E_{\text{corr}}$  to control at  $P = .05$  (Fig. 4C).

### 3.3. Electrochemical impedance spectroscopy (EIS)

EIS is a non-destructive corrosion test method that evaluates metal coatings or oxide layer that inherently builds on the metal surface (such as Ti oxide layer). EIS is used to assess the corrosion tendency of a metal. Nyquist and Bode plots were constructed using EIS data, and representative plots are presented in Fig. 5. Within TB groups, the Nyquist plot shows that TB8mm reduced the capacitance semi-loop the most (causing the most corrosion kinetics) followed by TB3mm and TB5mm compared to the control. FC8mm had the most corrosion kinetics in the FC groups, followed by FC5mm, FC3mm, and control. Within PC groups, the order capacitance semi-loop reduction PC8mm > PC5mm > PC3mm > control. Based on the Bode plot, TB at different amounts reduced the impedance, indicating more corrosion kinetics than control.

Similarly, different amounts of FC decreased the impedance and phase angle compared to the control, especially FC8mm. Finally, the increasing amount of PC decreased the impedance compared to the control. Comparing Nyquist (Fig. 5A) and Bode plots (Fig. 5B) of different cement types, FC reduced the capacitance semi-loop, impedance, and phase angle the most, followed by PC compared to control.

EIS data are commonly interpreted using an equivalent circuit. Modified Randle's circuit with a constant phase element (CPE) was applied in this study (Fig. 6A), from which  $R_p$  and  $C_{dl}$  were calculated. TB cement dropped  $R_p$  significantly compared to the control (Fig. 6B).  $C_{dl}$  did not exhibit any statistical differences for the types of cement (Fig. 6C).

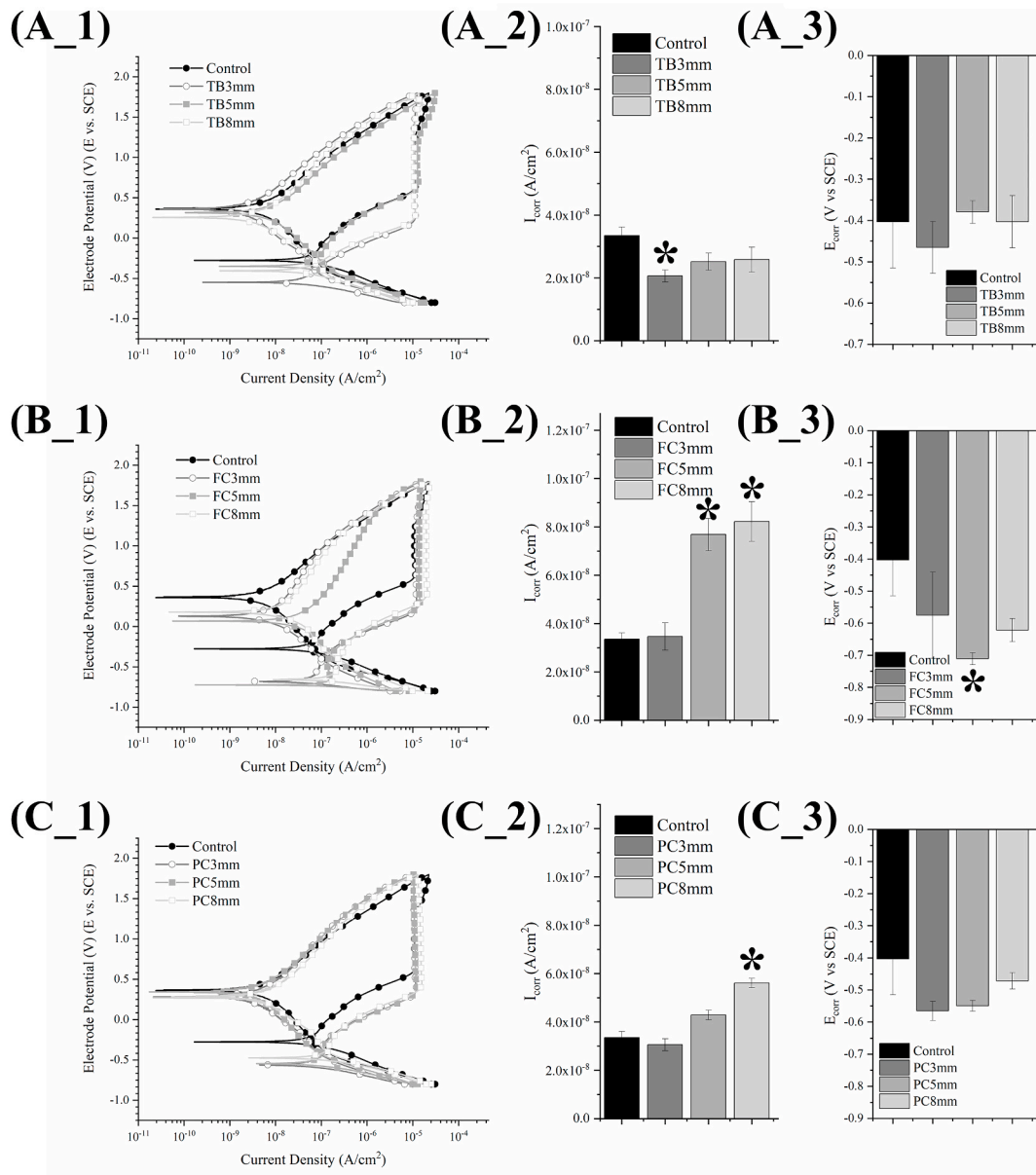


**Fig. 3.** A, potentiodynamic curves of the increasing TB cement amount from which  $i_{corr}$  and  $E_{corr}$  graphs were derived. B, potentiodynamic curves of three different amounts of FC cement and the corresponding  $i_{corr}$  and  $E_{corr}$  graphs. C, potentiodynamic curves of three different amounts of PC cement and the corresponding  $i_{corr}$  and  $E_{corr}$  graphs. In the graphs, the groups that have (\*) are statistically different compared to the control ( $p \leq .05$ ).

#### 3.4. Metal ion estimation through ICPMS

The ICPMS analysis revealed that TB cement did not increase Ti ion release into artificial saliva (Fig. 7A). On the contrary, there was a strong positive correlation between the amount of FC and PC cement and the Ti concentration in the electrolyte solution, with a correlation coefficient of 0.75 ( $P = .005$ ) and 0.71 ( $P = .009$ ), respectively (Fig. 7B and C). As a function of cement type, PC cement increased the Ti concentration the most, followed by FC compared to the control ( $P \leq .05$ ) (Fig. 7D). Additionally, the increasing amount of TB cement in artificial saliva increased the concentration of Zn ions with a correlation coefficient of 0.92 ( $P < .001$ ) (Fig. 7E).

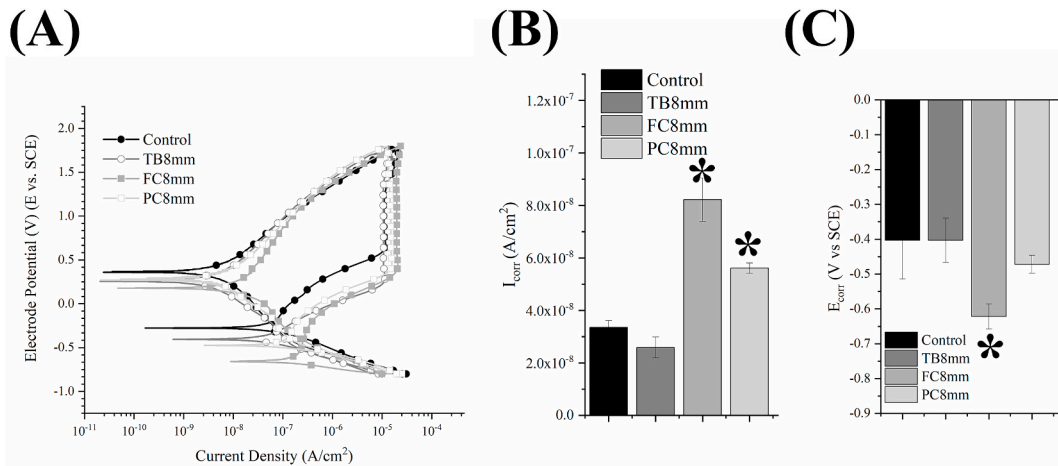


**Fig. 4.** A, representative potentiodynamic curves that compare cement types used in this study in terms of corrosion behavior. B,  $i_{corr}$  graph and C,  $E_{corr}$  graph derived from potentiodynamic curves. Groups that have (\*) are statistically different compared to the control ( $p \leq .05$ ).

**Table 3**

Means and standard deviations (SD) of  $i_{corr}$  (A/cm<sup>2</sup>) and  $E_{corr}$  (V) of all the experimental groups. (\*) indicated statistical significance compared to control.

Corrosion parameter	Cement amount	Cement type			
		Control (no cement)	TB	FC	PC
$i_{corr}$ (SD)	3 mm	$3.35 \times 10^{-8} (\pm 2.61 \times 10^{-9})$	$2.06 \times 10^{-8} (\pm 2.0 \times 10^{-9})$	$3.46 \times 10^{-8} (\pm 5.64 \times 10^{-9})$	$3.05 \times 10^{-8} (\pm 2.45 \times 10^{-9})$
	5 mm		$2.52 \times 10^{-8*} (\pm 2.73 \times 10^{-9})$	$7.68 \times 10^{-8*} (\pm 6.67 \times 10^{-9})$	$4.29 \times 10^{-8} (\pm 2.0 \times 10^{-9})$
	8 mm		$2.60 \times 10^{-8*} (\pm 4.0 \times 10^{-9})$	$8.22 \times 10^{-8*} (\pm 8.22 \times 10^{-9})$	$5.61 \times 10^{-8*} (\pm 1.93 \times 10^{-9})$
$E_{corr}$ (SD)	3 mm	-0.40 ( $\pm 0.11$ )	-0.47 ( $\pm 0.06$ )	-0.58 ( $\pm 0.13$ )	-0.57 ( $\pm 0.03$ )
	5 mm		-0.38 ( $\pm 0.03$ )	-0.71* ( $\pm 0.02$ )	-0.55 ( $\pm 0.02$ )
	8 mm		-0.40 ( $\pm 0.06$ )	-0.62 ( $\pm 0.04$ )	-0.47 ( $\pm 0.03$ )

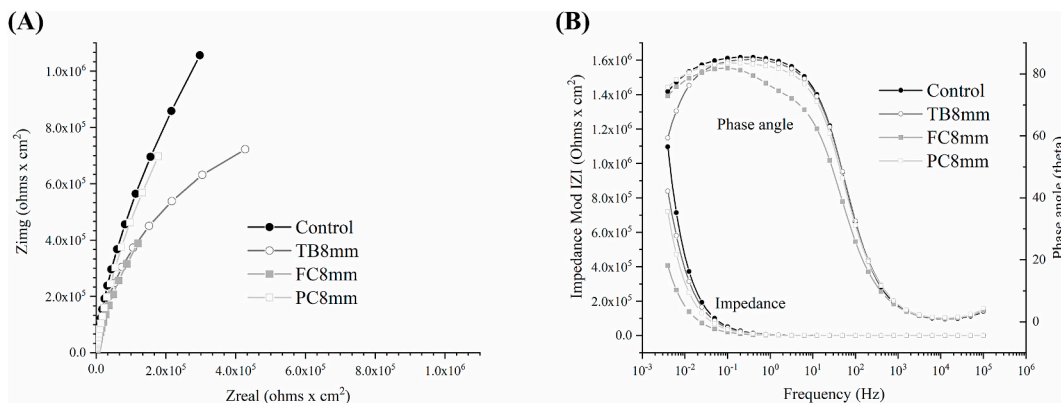


**Fig. 5.** A, representative Nyquist plots and B, Bode plots comparing the different cement types used in this study.

### 3.5. Evolution of pH

The artificial saliva pH was around 6.5 before adding any cement. At 30 min, TB caused a slight drop in pH to 6.19, which gradually increased to 6.3 at the remaining time points. FC pH readings dropped from 6.13 at 30 min to 5.98 at 4 h. Finally, PC dropped pH the most, and the pH readings were 5.75, 5.85, 5.84, and 5.87 at 30 min, 1 h, 2 h, and 4 h, respectively.

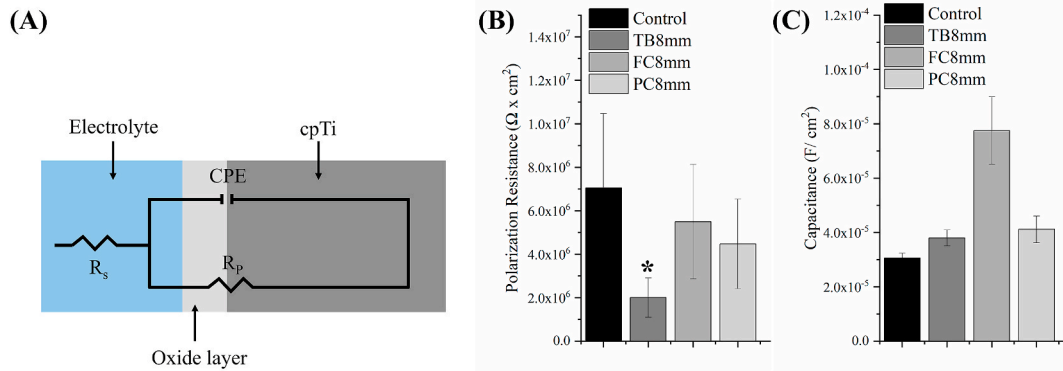


**Fig. 6.** A, schematic illustrating modified Randle's circuit. B,  $R_p$  graphs and C,  $C_{dl}$  graphs based on cement type. Groups that have (\*) are statistically different compared to the control ( $p \leq .05$ ).

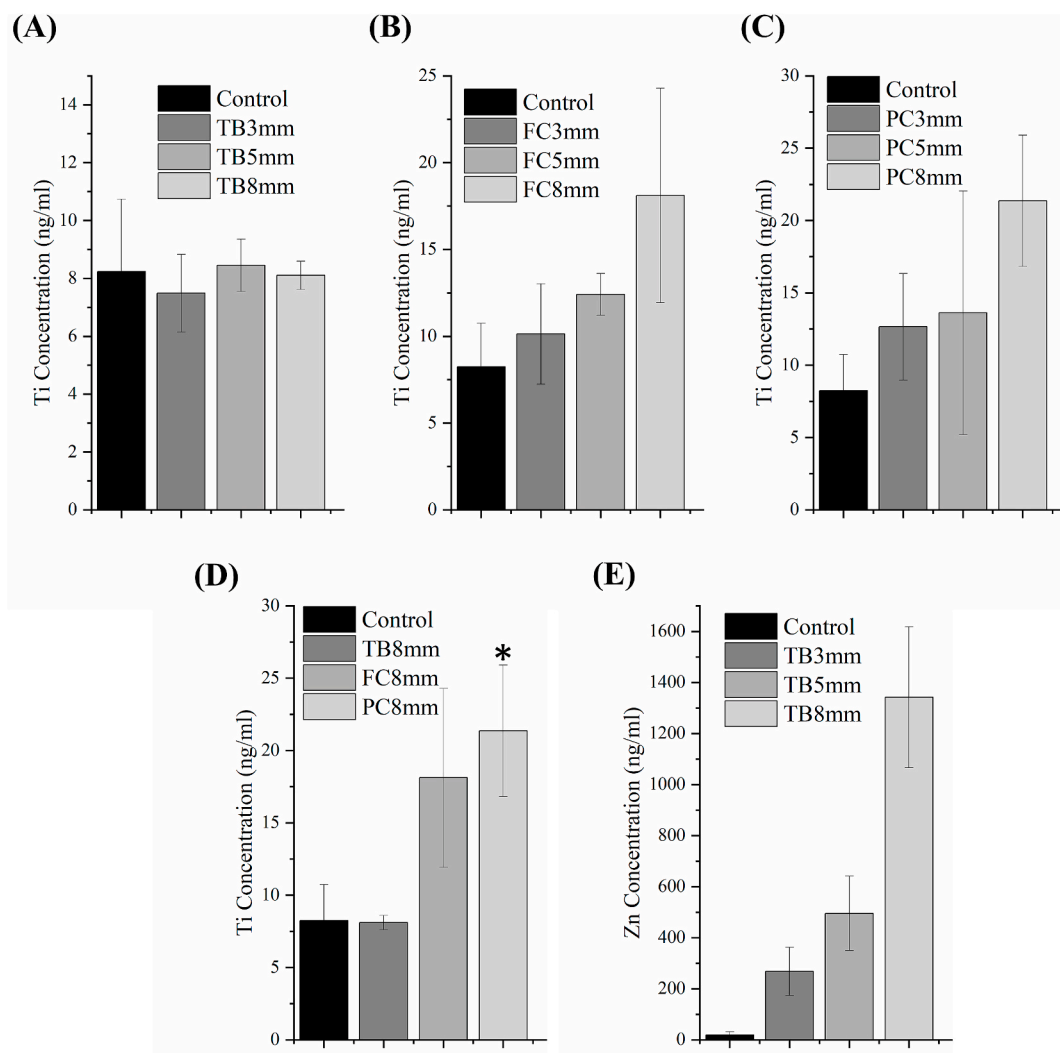


**Fig. 7.** ICPMS analysis of electrolyte solutions after corrosion. A-C Ti ion concentration based on cement amount and D, based on cement type. E, Zn ions concentration in TB cement group. Zn ions concentration increased as amount of TB cement increased.

### 3.6. Surface analysis

The first step in the surface analysis used a 3D white-light microscope to evaluate the differences between corroded and non-corroded surfaces of each sample (Fig. 8A–E). As shown in Fig. 9, the Ra values of corroded surfaces are higher than those of non-corroded surfaces, especially in TB3mm, FC, and PC groups. Further surface analysis with SEM (magnification = 3000×) generally revealed more surface irregularities in corroded surfaces compared to non-corroded surfaces (Fig. 10A–E). The final step in the surface analysis used EDS, which indicated the presence of O, C, and Ti in the corrosion area. Based on the limited number of the EDS spectra, it is revealed that FC8mm and PC5mm had more O percentage by weight (5.92% and 6.20%, respectively) (Fig. 11B\_1 and B\_2) than the control (4.75%) (Fig. 11A\_1 and A\_2), which may indicate more corrosion processes.

## 4. Discussion

The current study demonstrated that various dental cement amounts impacted Ti corrosion processes. FC and PC in higher amounts increased  $i_{\text{corr}}$ . Moreover, Ti corrosion levels varied with different cement types. More specifically, FC increased  $i_{\text{corr}}$  the most, followed by PC compared to control. To the best of our knowledge, this is the first study that demonstrated the impact of dental cement amount on Ti corrosion.

The first cement type is non-eugenol zinc oxide cement (TB), which is used for temporary cementation. Using such temporary cement is not uncommon in implant dentistry, especially for the cementation of temporary implant crowns and even permanent cementation [25,26]. The second and third types of cement used in this study were resin-based cement, FC and PC, considered permanent cement. The micro-shear bond strength of PC ( $\approx 26.5$  MPa) to CP Ti was found to be more than double the strength of FujiCEM II ( $\approx 8.5$  MPa) [27].

Results indicate that FC had the highest  $i_{\text{corr}}$  among the other cement types, which increased at higher amounts. FC is a resin-modified glass ionomer, a restorative/cement family that has the inherent feature of fluoride release [28,29]. One study found that the fluoride release from glass ionomer was around 25 ppm within the first 24 h after cement setting and about 5 ppm after three weeks [30]. The negative influence of fluoride on Ti corrosion is well established [31,32]. Suggested is that fluoride may damage the oxide layer by forming a soluble Ti–F compound ( $\text{Na}_2\text{TiF}_6$ ,  $\text{TiCl}_6$ , and/or  $\text{TiF}_6$ ), leading to a significant reduction in corrosion resistance [32, 33]. For example, a study examined the impact of different concentrations of fluoride (i.e. 0, 20, 30, 12,300 ppm) on commercially pure titanium grade 4 and TiAl6V4 alloy found a significant drop in corrosion resistance in high corrosion concentration [34]. Despite the initial increase of fluoride release, it is worth to note that it can reduce exponentially over a week and therefore, the corrosion results might vary. Another study postulated that the presence of high concentrations of fluoride in the vicinity of Ti surface leads to surface activation by hindering the formation of the oxide layer, making the surface more susceptible to corrosion [35]. It is worth noting that one study found no significant difference in terms of cytotoxicity of human gingival fibroblast and MC3T3-E1 preosteoblast cells between the sample containing fluoride-releasing cements and fluoride releasing-cement placed on Ti surface [36]. However, the

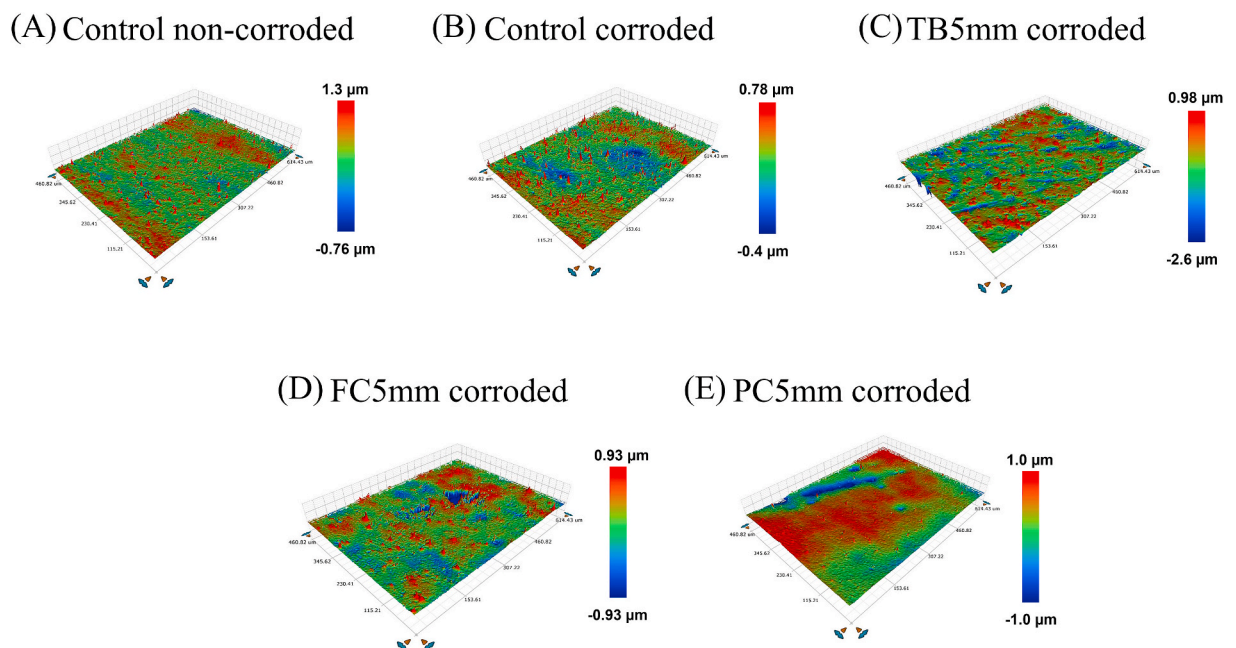


**Fig. 8.** Representative 3D white light microscopic images of the sample surface of A, control before corrosion, B, control after corrosion, C, TB after corrosion, D, FC after corrosion, and E, PC after corrosion.

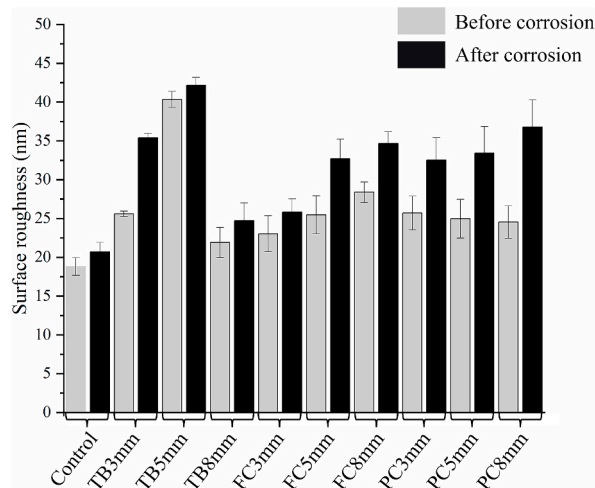


Fig. 9. Surface roughness (in nm) of representative samples before and after corrosion.

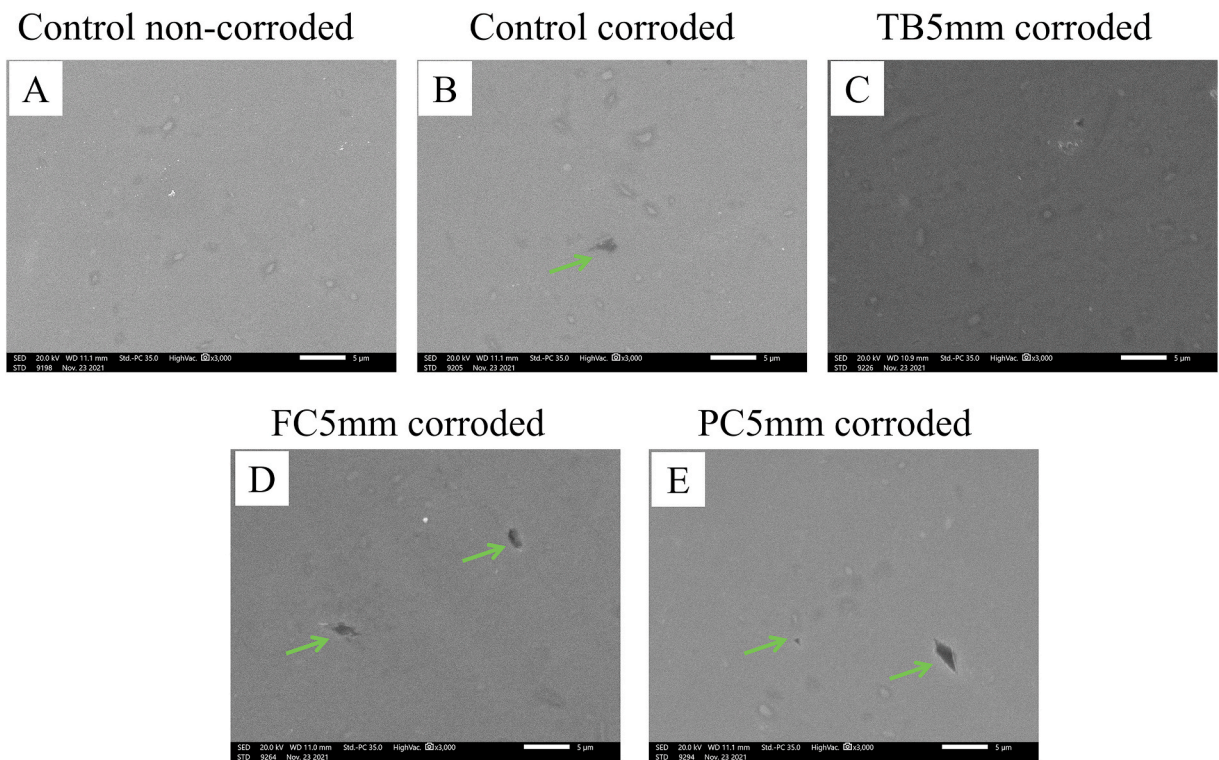
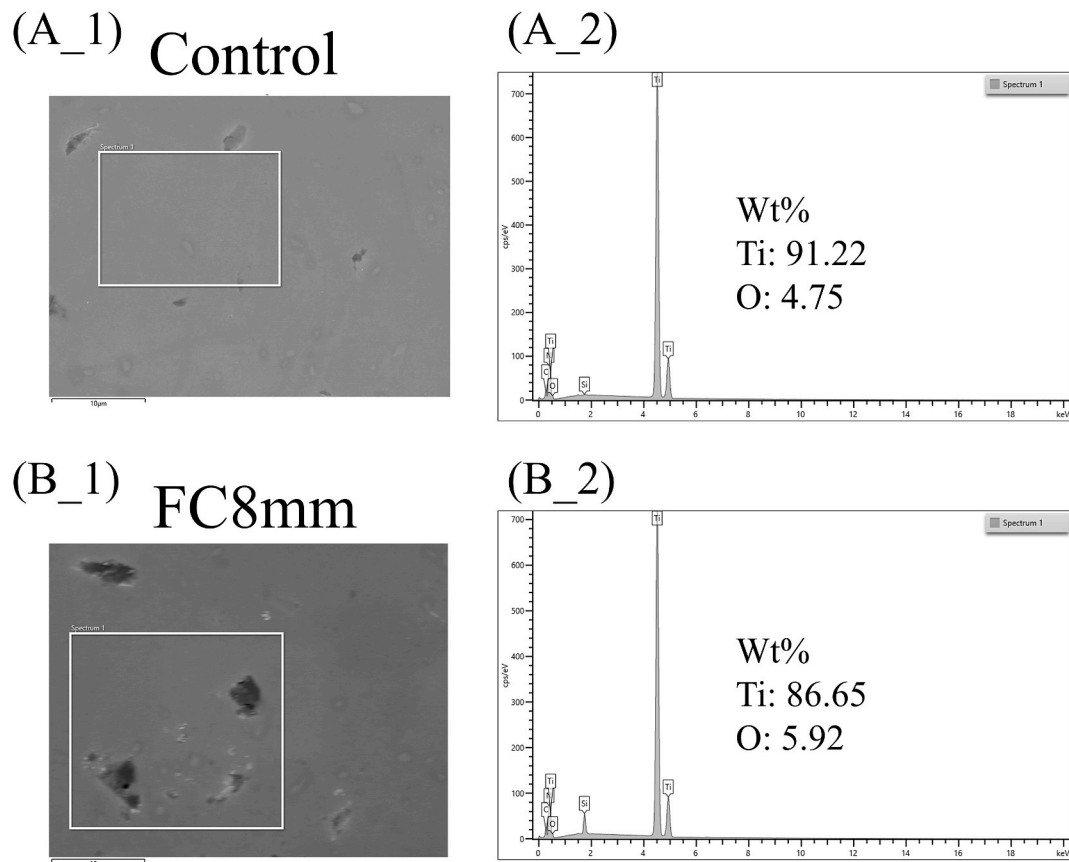


Fig. 10. Representative SEM images at 3000 $\times$  magnification of sample surface of A, control before corrosion, B, control after corrosion, C, TB after corrosion, D, FC after corrosion, and E, PC after corrosion. The green arrows indicate the surface damage from the corrosion process.

time the cells were exposed to the cement/titanium group might be very short (24 h) to cause a significant corrosion. Alternatively, a longer period or applying accelerated corrosion protocols might show different results.

In the current study, PC is the second most cement to enhance  $i_{\text{CORR}}$ , which increased when the cement amount was higher. Based on the pH measurements, PC had the lowest pH readings throughout the corrosion experiment (4 h). Low pH values have been found to increase the corrosion processes of CP Ti [13,37]. A previous study investigated the effect of different pH levels (pH = 3, 6.5, and 9) on commercially pure titanium grade 4 and TiAl6V4 alloy and found that low pH levels increased the corrosion rate and decreased corrosion resistance compared. Additionally, based on potentiodynamic curves, the negative hysteresis indicates that the Ti surface underwent repassivation, leaving the oxide layer intact under all tested conditions.

On the contrary, TB decreased  $i_{\text{CORR}}$  compared to control. The preparation of TB involves the mixture of two pastes, base, and



**Fig. 11.** A, EDS spectrum of control and B, FC8mm after corrosion. On FC8mm sample corroded surface, more oxygen was detected in terms of weight percentage compared to control, indicating more corrosion processes.

catalyst. 60–100% of the base paste contains zinc oxide. Based on ICPMS analysis, Zn concentration increased as the amount of TB cement increased. Zinc oxide was found to increase the corrosion resistance and decrease the amount of Ti ions released when used as a coating material on Ti6Al4V [38]. Although this cannot be applied directly to our study, zinc oxide might protect the Ti surface and decrease the corrosion processes.

In the current study, Nyquist and Bode plots of TB indicate that as the amount of TB cement increased, the capacitance semi-loop, impedance, and phase angle decreased, indicating more corrosion kinetics, in contrast  $i_{corr}$  data. EIS tests were performed at the general stable potential of the material (EOS) to study the local corrosion kinetics. TB groups might show different trends if EIS is performed at different potentials, which is not within the scope of this study. Moreover, based on Nyquist and Bode plots, the other two types of cement increased corrosion kinetics, possibly because of the increase of fluoride concentration in case of FC, and pH drop in case of PC, causing more corrosion kinetics. Previous studies demonstrated that lower pH values and fluoride in contact with Ti surface reduced the corrosion resistance [15,39,40].

To understand the local kinetics at the solution-titanium interface, an equivalent electrical circuit was developed to obtain  $R_p$  and  $C_{dl}$ , revealing Ti surface's oxide layer properties [41]. Decreased  $R_p$  and corresponding increased  $C_{dl}$  indicate more corrosion kinetics. Comparing the three cement types, FC increased  $C_{dl}$  the most compared to the other groups. Higher  $C_{dl}$  values indicate that the metal has more capacity to exchange ions in the electrochemical environment [13], which FC elicited in this study.

The current study examined the sample surface under a 3D white microscope, SEM, and EDS to confirm the electrochemical data.  $R_a$  values of corroded surfaces were generally higher compared to non-corroded surfaces. Moreover, based on the limited number of the EDS spectra, FC8mm and PC5mm have the highest oxygen percentage by weight (5.92% and 6.20%, respectively) on the corroded surface compared to the control (4.75%). The higher percentage of surface oxygen may reflect the increased corrosion processes. A previous study that tested the effect of Ti particles and ions on the corrosion process of commercially pure Ti grade 2 reached the same conclusion [42].

In the current study, three cement amounts were used to test the effect on corrosion at different quantities. These amounts were selected based on the assumption that 2 mm of excess cement is left around a 6 mm-diameter dental implant, and the calculation of the surface area covered by the cement resulted in 37.68 mm<sup>2</sup>. The corresponding circle surface area on the sample (Ti disc) is achieved when a 7 mm-punch biopsy tool is used. On this basis, a small surface area (3 mm-punch biopsy), a large surface area (8 mm-punch biopsy), and a surface area in the middle (5 mm-punch biopsy) were selected (Fig. 1A). In a clinical scenario, not only could the

undetected excess cement irritate the peri-implant tissues, but certain types of cement can accelerate Ti corrosion, resulting in an additional potential risk of increased inflammation (Fig. 12). Residual cement was associated with peri-implant disease [9,10,43,44], and higher levels of Ti products were found around diseased implants [6,45,46]. In contrast, other types of cement, such as TB could reduce the Ti corrosion activity, as the current study demonstrated. In one study, TB was associated with inflammation relief when it was used to cement the crowns of inflamed dental implants due to excess methacrylate cement [7].

The current study has several limitations that will be considered in the future. The samples were only exposed to one condition - cement. Future studies will aim to explore the combined effect of several conditions on Ti corrosion, in addition to cement. Additionally, the tests were performed on mirror-shine polished Ti discs, whereas most dental implant surfaces are not polished. Future research will involve the use of actual dental implants. Furthermore, future experiments will be planned to study in-depth corrosion kinetics and mechanisms.

Another limitation is that the metal ion results may not represent the normal conditions, as the samples were subjected to anodic electrochemical conditions. Also, the interactions between the metallic ions were not included in this study. Furthermore, The present work did not investigate the microstructure variability, which might have an influence on the corrosion results. Regarding SEM and white-light microscopy, direct comparison between the images from imaging techniques might not be possible, due to the possibility of differences between the scanned areas using these imaging techniques.

It is worth noting that the corrosion tests were performed 5 min following the setting of the cement, and the effect of the delayed cement setting was not considered. Finally, this study did not take into account the mechanical aspect (tribology), and upcoming research will investigate the combined effect of corrosion and tribology (tribocorrosion) on the Ti surface to simulate the oral environment better.

From the clinical perspective, clinicians may need to consider the effect of cement on Ti dissolution in their decision-making. Screw-retained crown is a good alternative to a cement-retained crown to avoid the potential risk of biological complications [47]. If cement-retained crown is necessary, it might be worth considering the cementation technique and cement type to reduce the risk of excess cement. For example, a systematic review concluded that extraoral implant crown cementation can significantly reduce the amount of excess cement. In addition, zinc-oxide cement, including eugenol-free, seems to have an advantage over the other cement types, when used to for implant crowns [48].

## 5. Conclusions

The main conclusions of this study are as follows. Both FC and PC increased the corrosion rate and kinetics when in contact with Ti surface at higher amounts. The amount of FC and PC is directly proportional to the Ti ion concentration due to Ti corrosion. Further studies are required to explore the role of cement on implant corrosion.

## Clinical implications

Cement-retained implant prostheses are commonly used in dental practice. Choosing cement and meticulously applying the right amount of cement might be crucial in mitigating the risk of Ti corrosion and undetected excess cement.

## Data availability

The study data has not been deposited into a publicly available repository. The data will be available upon request.

## CRediT authorship contribution statement

**Mostafa Alhamad:** Conceptualization, Data curation, Formal analysis, Investigation, Methodology, Project administration, Resources, Supervision, Validation, Visualization, Writing – original draft, Writing – review & editing. **Valentim A.R. Barão:** Conceptualization, Supervision, Writing – review & editing. **Cortino Sukotjo:** Conceptualization, Supervision, Writing – review & editing,

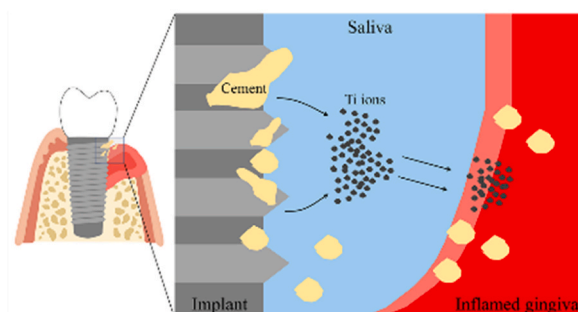


Fig. 12. Schematic diagram of the cement acceleration of corrosion and contribution to the peri-implantitis risk.

Resources. **Mathew T. Mathew:** Conceptualization, Funding acquisition, Investigation, Resources, Supervision, Writing – review & editing.

## Declaration of competing interest

The authors declare the following financial interests/personal relationships which may be considered as potential competing interests: Dr. Valentim Barao is a co-author of this manuscript and he is a co-editor of Heliyon.

## References

- [1] T. Berglundh, G. Armitage, M.G. Araujo, G. Avila-Ortiz, J. Blanco, P.M. Camargo, S. Chen, D. Cochran, J. Derks, E. Figuero, C.H.F. Hämmeler, L.J.A. Heitz-Mayfield, G. Huynh-Ba, V. Iacono, K.-T. Koo, F. Lambert, L. McCauley, M. Quirynen, S. Renvert, G.E. Salvi, F. Schwarz, D. Tarnow, C. Tomasi, H.-L. Wang, N. Zitzmann, Peri-implant diseases and conditions: consensus report of workgroup 4 of the 2017 World Workshop on the classification of periodontal and peri-implant diseases and conditions, *J. Periodontol.* 89 (2018) S313–S318, <https://doi.org/10.1002/JPER.17-0739>.
- [2] M.D. Soler, S.-M. Hsu, C. Fares, F. Ren, R.J. Jenkins, L. Gonzaga, A.E. Clark, E. O'Neill, D. Neal, J.F. Esquivel-Upshaw, Titanium corrosion in peri-implantitis, *Materials* 13 (2020) 5488, <https://doi.org/10.3390/ma13235488>.
- [3] Z. Berryman, L. Bridger, H.M. Hussaini, A.M. Rich, M. Atieh, A. Tawse-Smith, Titanium particles: an emerging risk factor for peri-implant bone loss, *Saudi Dent. J.* 32 (2020) 283–292, <https://doi.org/10.1016/j.sdentj.2019.09.008>.
- [4] G.O. Alrabeah, P. Brett, J.C. Knowles, H. Petridis, The effect of metal ions released from different dental implant-abutment couples on osteoblast function and secretion of bone resorbing mediators, *J. Dent.* 66 (2017) 91–101, <https://doi.org/10.1016/j.jdent.2017.08.002>.
- [5] L.M. Safioti, G.A. Kotsakis, A.E. Pozhitkov, W.O. Chung, D.M. Daubert, Increased levels of dissolved titanium are associated with peri-implantitis - a cross-sectional study, *J. Periodontol.* 88 (2017) 436–442, <https://doi.org/10.1902/jop.2016.160524>.
- [6] T. Fretwurst, G. Buzanich, S. Nahles, J.P. Woelber, H. Riesemeier, K. Nelson, Metal elements in tissue with dental peri-implantitis: a pilot study, *Clin. Oral Implants Res.* 27 (2016) 1178–1186, <https://doi.org/10.1111/clr.12718>.
- [7] M. Korsch, U. Obst, W. Walther, Cement-associated peri-implantitis: a retrospective clinical observational study of fixed implant-supported restorations using a methacrylate cement, *Clin. Oral Implants Res.* 25 (2014) 797–802, <https://doi.org/10.1111/clr.12173>.
- [8] M. Korsch, W. Walther, A. Bartols, Cement-associated peri-implant mucositis. A 1-year follow-up after excess cement removal on the peri-implant tissue of dental implants, *Clin. Implant Dent. Relat. Res.* 19 (2017) 523–529.
- [9] T.G. Wilson, The positive relationship between excess cement and peri-implant disease: a prospective clinical endoscopic study, *J. Periodontol.* 80 (2009) 1388–1392, <https://doi.org/10.1902/jop.2009.090115>.
- [10] T. Linkevicius, A. Puisys, E. Vindasiute, L. Linkeviciene, P. Apse, Does residual cement around implant-supported restorations cause peri-implant disease? A retrospective case analysis, *Clin. Oral Implants Res.* 24 (2013) 1179–1184, <https://doi.org/10.1111/j.1600-0501.2012.02570.x>.
- [11] G. Manivasagam, D. Dhinasekaran, A. Rajamanickam, Biomedical implants: corrosion and its prevention - a review, *Recent Pat. Corros. Sci.* 2 (2010).
- [12] M.T. Mathew, V.A. Barão, J.C.-C. Yuan, W.G. Assunção, C. Sukoito, M.A. Wimmer, What is the role of lipopolysaccharide on the tribocorrosive behavior of titanium? *J. Mech. Behav. Biomed. Mater.* 8 (2012) 71–85, <https://doi.org/10.1016/j.jmbmb.2011.11.004>.
- [13] V.A.R. Barão, M.T. Mathew, W.G. Assunção, J.C.-C. Yuan, M.A. Wimmer, C. Sukoito, Stability of cp-Ti and Ti-6Al-4V alloy for dental implants as a function of saliva pH - an electrochemical study, *Clin. Oral Implants Res.* 23 (2012) 1055–1062, <https://doi.org/10.1111/j.1600-0501.2011.02265.x>.
- [14] D.G. Olmedo, G. Nalli, S. Verdú, M.L. Paparella, R.L. Cabrini, Exfoliative cytology and titanium dental implants: a pilot study, *J. Periodontol.* 84 (2013) 78–83, <https://doi.org/10.1902/jop.2012.110757>.
- [15] D.C. Rodrigues, P. Valderrama, T.G. Wilson, K. Palmer, A. Thomas, S. Sridhar, A. Adapalli, M. Burbano, C. Wadhvani, Titanium corrosion mechanisms in the oral environment: a retrieval study, *Materials* 6 (2013) 5258–5274, <https://doi.org/10.3390/ma6115258>.
- [16] A. Makke, A. Homs, M. Guzaiz, A. Almalki, Survey of screw-retained versus cement-retained implant restorations in Saudi Arabia, *Int. J. Dent.* 2017 (2017), 5478371, <https://doi.org/10.1155/2017/5478371>.
- [17] D.M. Daubert, B.F. Weinstein, S. Bordin, B.G. Leroux, T.F. Flemming, Prevalence and predictive factors for peri-implant disease and implant failure: a cross-sectional analysis, *J. Periodontol.* 86 (2015) 337–347, <https://doi.org/10.1902/jop.2014.140438>.
- [18] K. Karlsson, J. Derks, J. Håkansson, J.L. Wennström, M. Molin Thorén, M. Petzold, T. Berglundh, Technical complications following implant-supported restorative therapy performed in Sweden, *Clin. Oral Implants Res.* 29 (2018) 603–611, <https://doi.org/10.1111/clr.13271>.
- [19] M. Korsch, B.-P. Robra, W. Walther, Cement-associated signs of inflammation: retrospective analysis of the effect of excess cement on peri-implant tissue, *Int. J. Prosthodont.* (IJP) 28 (2015) 11–18, <https://doi.org/10.11607/ijp.4043>.
- [20] F. Demirel, G. Saygili, S. Sahmali, Corrosion susceptibility of titanium covered by dental cements, *J. Oral Rehabil.* 30 (2003) 1162–1167, <https://doi.org/10.1111/j.1365-2842.2003.01568.x>.
- [21] Y.L. Turpin, R.D. Tardivel, A. Tallec, A.C. Le Menn, Corrosion susceptibility of titanium covered by dental cements, *Dent. Mater.* 16 (2000) 57–61, [https://doi.org/10.1016/s0109-5641\(99\)00087-1](https://doi.org/10.1016/s0109-5641(99)00087-1).
- [22] J.N. Saba, D.A. Siddiqui, L.C. Rodriguez, S. Sridhar, D.C. Rodrigues, Investigation of the corrosive effects of dental cements on titanium, *J. Bio. Tribo. Corr.* 3 (2017) 25.
- [23] C.P.K. Wadhvani, Peri-implant disease and cemented implant restorations: a multifactorial etiology, *Compend Contin Educ Dent.* (2013) 32–37, 34 Spec No 7.
- [24] C. Wadhvani, T. Hess, A. Piñeyro, R. Opler, K.-H. Chung, Cement application techniques in luting implant-supported crowns: a quantitative and qualitative survey, *Int. J. Oral Maxillofac. Implants* 27 (2012) 859–864.
- [25] E. Frisch, P. Ratka-Krüger, P. Weigl, J. Woelber, Extraoral cementation technique to minimize cement-associated peri-implant marginal bone loss: can a thin layer of zinc oxide cement provide sufficient retention? *Int. J. Prosthodont.* (IJP) 29 (2016) 360–362, <https://doi.org/10.11607/ijp.4599>.
- [26] N. Almeahadi, A. Kutkut, M. Al-Sabbagh, What is the best available luting agent for implant prosthesis? *Dent. Clin.* 63 (2019) 531–545, <https://doi.org/10.1016/j.cden.2019.02.014>.
- [27] M. Nakhaei, Z. Fendereski, S. Alavi, H.-S. Mohammadipour, The Micro-Shear bond strength of different cements to commercially pure titanium, *J. Clin. Exp. Dent.* 11 (2019) e820–e828, <https://doi.org/10.4317/jced.56022>.
- [28] F.M. Burke, N.J. Ray, R.J. McConnell, Fluoride-containing restorative materials, *Int. Dent. J.* 56 (2006) 33–43, <https://doi.org/10.1111/j.1875-595x.2006.tb00072.x>.
- [29] L. Forsten, Fluoride release and uptake by glass ionomers, *Scand. J. Dent. Res.* 99 (1991) 241–245, <https://doi.org/10.1111/j.1600-0722.1991.tb01891.x>.
- [30] L. Forsten, Short- and long-term fluoride release from glass ionomers and other fluoride-containing filling materials in vitro, *Scand. J. Dent. Res.* 98 (1990) 179–185, <https://doi.org/10.1111/j.1600-0722.1990.tb00958.x>.
- [31] J. Noguti, F. de Oliveira, R.C. Peres, A.C.M. Renno, D.A. Ribeiro, The role of fluoride on the process of titanium corrosion in oral cavity, *Biometals* 25 (2012) 859–862, <https://doi.org/10.1007/s10534-012-9570-6>.
- [32] E.M. Anwar, L.S. Kheiralla, R.H. Tammam, Effect of fluoride on the corrosion behavior of Ti and Ti6Al4V dental implants coupled with different superstructures, *J. Oral Implantol.* 37 (2011) 309–317, <https://doi.org/10.1563/AAID-JOI-D-09-00084>.
- [33] H.-H. Huang, T.-H. Lee, Electrochemical impedance spectroscopy study of Ti-6Al-4V alloy in artificial saliva with fluoride and/or bovine albumin, *Dent. Mater.* 21 (2005) 749–755, <https://doi.org/10.1016/j.dental.2005.01.009>.

- [34] J.C. Souza, S.L. Barbosa, E.A. Ariza, M. Henriques, W. Teughels, P. Ponthiaux, J.-P. Celis, L.A. Rocha, How do titanium and Ti6Al4V corrode in fluoridated medium as found in the oral cavity? An in vitro study, *Mater. Sci. Eng. C* 47 (2015) 384–393.
- [35] F. Rosalbino, S. Delsante, G. Borzone, G. Scavino, Influence of noble metals alloying additions on the corrosion behaviour of titanium in a fluoride-containing environment, *J. Mater. Sci. Mater. Med.* 23 (2012) 1129–1137, <https://doi.org/10.1007/s10856-012-4591-9>.
- [36] J.C. Marvin, S.I. Gallegos, S. Parsaei, D.C. Rodrigues, In vitro evaluation of cell compatibility of dental cements used with titanium implant components, *J. Prosthodont.* 28 (2019) e705–e712.
- [37] M. Koike, H. Fujii, The corrosion resistance of pure titanium in organic acids, *Biomaterials* 22 (2001) 2931–2936, [https://doi.org/10.1016/S0142-9612\(01\)00040-0](https://doi.org/10.1016/S0142-9612(01)00040-0).
- [38] A. Woźniak, W. Walke, A. Jakóbk-Kolon, B. Ziębowicz, Z. Brytan, M. Adamiak, The influence of ZnO oxide layer on the physicochemical behavior of Ti6Al4V titanium alloy, *Materials* 14 (2021) 230, <https://doi.org/10.3390/ma14010230>.
- [39] S. Takemoto, M. Hattori, M. Yoshinari, E. Kawada, Y. Oda, Corrosion behavior and surface characterization of titanium in solution containing fluoride and albumin, *Biomaterials* 26 (2005) 829–837, <https://doi.org/10.1016/j.biomaterials.2004.03.025>.
- [40] G. Mabileau, S. Bourdon, M.L. Joly-Guillou, R. Filmon, M.F. Baslé, D. Chappard, Influence of fluoride, hydrogen peroxide and lactic acid on the corrosion resistance of commercially pure titanium, *Acta Biomater.* 2 (2006) 121–129, <https://doi.org/10.1016/j.actbio.2005.09.004>.
- [41] L.P. Faverani, V.A.R. Barao, M.F.A. Pires, J.C.-C. Yuan, C. Sukotjo, M.T. Mathew, W.G. Assunção, Corrosion kinetics and topography analysis of Ti-6Al-4V alloy subjected to different mouthwash solutions, *Mater. Sci. Eng., C* 43 (2014) 1–10, <https://doi.org/10.1016/j.msec.2014.06.033>.
- [42] M. Alhamad, V.A.R. Barão, C. Sukotjo, L.F. Cooper, M.T. Mathew, Ti-ions and/or particles in saliva potentially aggravate dental implant corrosion, *Materials* 14 (2021) 5733, <https://doi.org/10.3390/ma14195733>.
- [43] P. Pesce, L. Canullo, M.G. Grusovin, H. de Bruyn, J. Cosyn, P. Pera, Systematic review of some prosthetic risk factors for periimplantitis, *J. Prosthet. Dent* 114 (2015) 346–350, <https://doi.org/10.1016/j.prosdent.2015.04.002>.
- [44] L.J.A. Heitz-Mayfield, G.E. Salvi, Peri-implant mucositis, *J. Clin. Periodontol.* 45 (Suppl 20) (2018) S237–S245, <https://doi.org/10.1111/jcpe.12953>.
- [45] T.G. Wilson Jr., P. Valderrama, M. Burbano, J. Blansett, R. Levine, H. Kessler, D.C. Rodrigues, Foreign bodies associated with peri-implantitis human biopsies, *J. Periodontol.* 86 (2015) 9–15, <https://doi.org/10.1902/jop.2014.140363>.
- [46] M. Petttersson, J. Petttersson, A. Johansson, M. Molin Thorén, Titanium release in peri-implantitis, *J. Oral Rehabil.* 46 (2019) 179–188.
- [47] J.-G. Witteben, T. Joda, H.-P. Weber, U. Brägger, Screw retained vs. cement retained implant-supported fixed dental prosthesis, *Periodontol.* 2000 73 (2017) 141–151, <https://doi.org/10.1111/prd.12168>.
- [48] R. Reda, A. Zanza, A. Cicconetti, S. Bhandi, R. Guarnieri, L. Testarelli, D. Di Nardo, A systematic review of cementation techniques to minimize cement excess in cement-retained implant restorations, *Methods Protoc* 5 (2022) 9, <https://doi.org/10.3390/mps5010009>.